Electronic Supplementary Material (ESI) for Polymer Chemistry.
This journal is © The Royal Society of Chemistry 2017

Electronic Supplementary Information

Ratiometric imaging of lysosomal hypochloric acid enabled by FRET-based polymer dots

Hong Wang, Peisheng Zhang,* Yongxiang Hong, Bin Zhao, Pinggui Yi and Jian Chen*

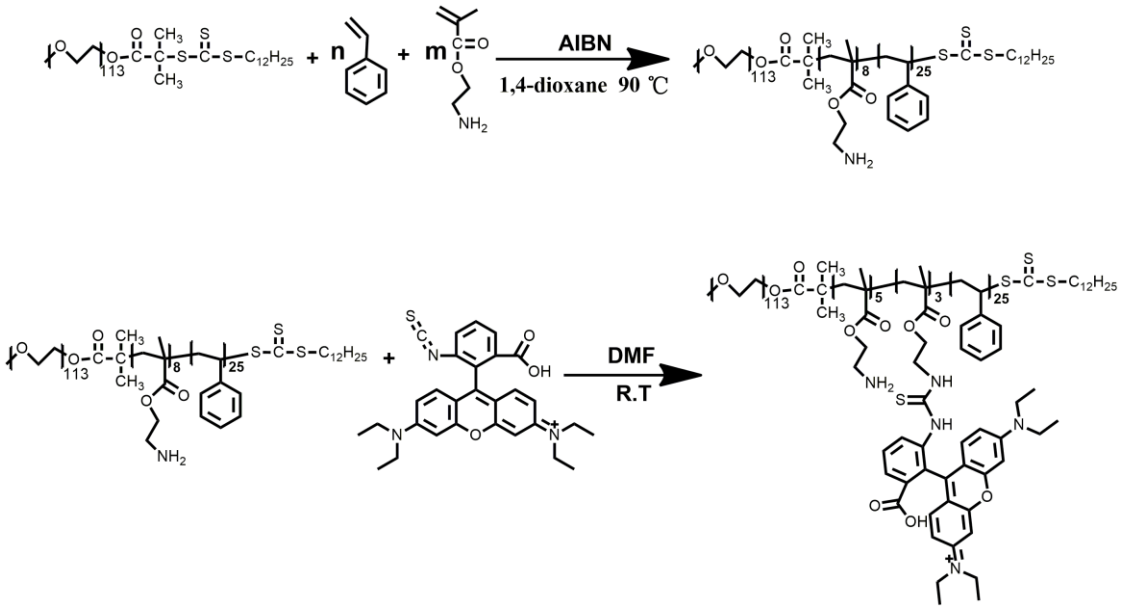

Scheme S1. Synthetic route of the probe **PEO_{113}-*b*-P(AEMH_5-*co*-AEMR_3-*co*-St_{25})**.

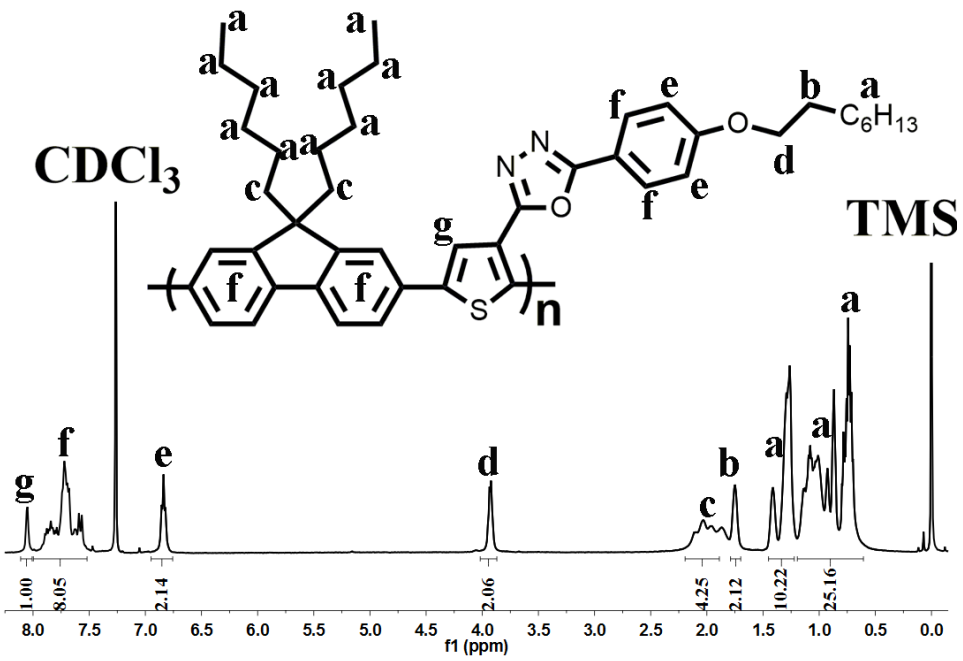

Figure S1. ^{1}H-NMR spectrum (in $CDCl_3$) of **PTPO**.

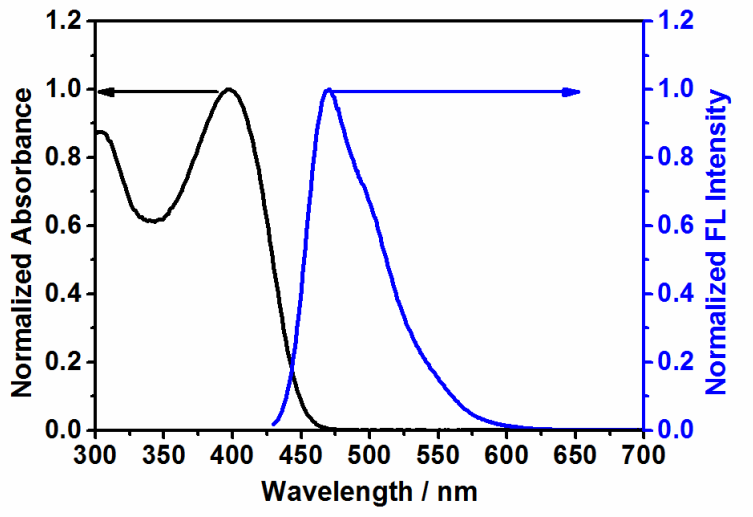

Figure S2. Normalized absorption and fluorescence emission spectra of **FPD** (FPD-1) in pH 5.0 PBS buffered water.

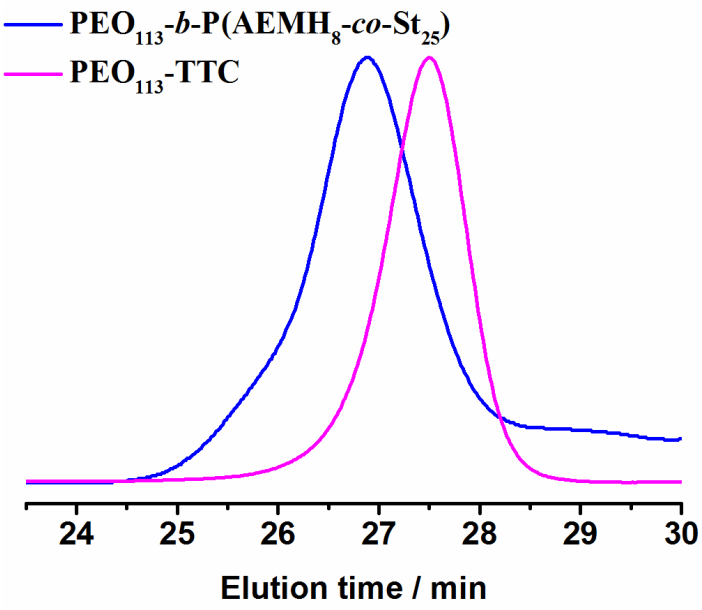

Figure S3. GPC trace of **PEO_{113}-TTC, PEO_{113}-*b*-P($AEMH_8$-*co*-St_{25})**

Table S1. Molecular weight distribution data of starting linear polymers.

Sample	$M_{n,GPC}$[a]	$M_{w,GPC}$[a]	PDI
PEO_{113}-TTC	8457	8944	1.06
PEO_{113}-*b*-P(AEMH$_8$-*co*-St$_{25}$)	12141	13741	1.12

[a]The data were acquired using SEC based on a polystyrene calibration curve and obtained from GPC analysis was using THF as eluent at a flow rate of 1.0 mL/min.

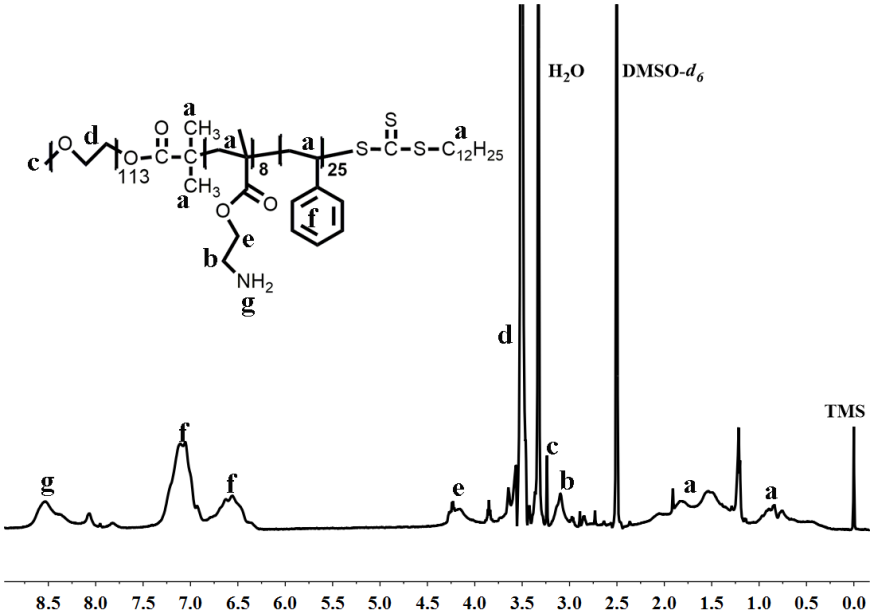

Figure S4. ^{1}H-NMR spectrum (in d_6-DMSO) of **PEO_{113}-*b*-P(AEMH_8-*co*-St_{25})**.

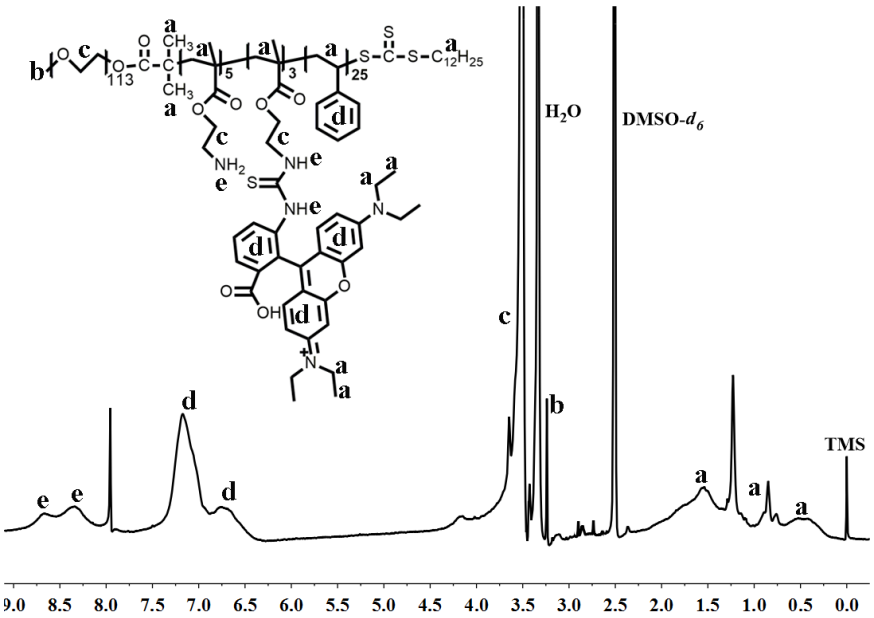

Figure S5. ^{1}H-NMR spectrum (in d_6-DMSO) of **PEO_{113}-*b*-P(AEMH_5-*co*-AEMR_3-*co*-St_{25})**.

Table S2. List of some data and parameters for two dye-incorporated nanoparticle samples

Sample[a]	Dye feed [10^{-2} mg ($\times10^{-9}$ mol)]		Dye feed [10^{-2} mg ($\times10^{-7}$ mol)]		Size[d] (nm)	Zeta Potential[e]
	PTPO	Determind[b]	RHB	Determind[c]		
FPD-0	0	0	0	0	31	7.2
FPD-1	12.00 (8.00)	11.13 (7.42)	0	0	27	7.8
FPD-2	0	0	14.20 (2.97)	13.34 (2.78)	35	4.8
FPD-3	12.00 (8.00)	11.32 (7.54)	14.20 (2.97)	13.55 (2.83)	29	5.6

[a]The PEO_{113}-*b*-P($AEMH_5$-*co*-$AEMR_3$-*co*-St_{25}) or PEO_{113}-*b*-P($AEMH_8$-*co*-St_{25}) feed is 1.2 mg, the PTPO feed is 0.12 mg, H_2O feed is 10 mL;

[b]Calculated by using the absorbance of PTPO at 395 nm in nanoparticle dispersion (eliminate the effect of scattering light) and the molar extinction coefficient of PTPO in dichloromethane, (ε = 890700 $mol^{-1}\cdot L\cdot cm^{-1}$);

[c]Calculated by using the absorbance of RHB at 554 nm in nanoparticle dispersion (eliminate the effect of scattering light) and the molar extinction coefficient of RHB in water (pH 5.0), (ε = 48000 $mol^{-1}\cdot L\cdot cm^{-1}$);

[d]Average diameter of nanoparticles were determined from DLS data;

[e]Zeta potential of nanoparticles were determined from DLS data.

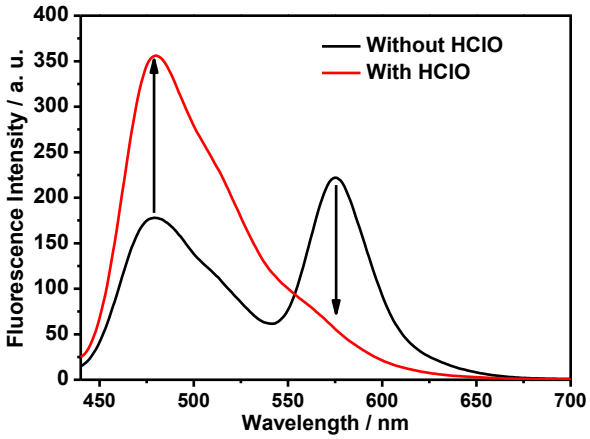

Figure S6. Fluorescence spectra of **FPD** (FPD-3, 12 μg/mL) in pH 5.0 PBS buffered water without and with HClO (7.0 μM, λ_{ex} = 420 nm).

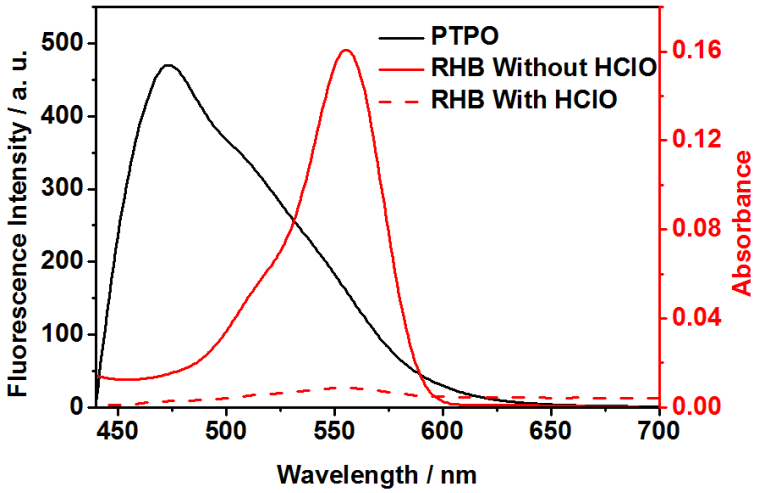

Figure S7. Fluorescence emission spectrum of **FPD** (FPD-1, black solid curve) and absorption spectrum of **FPD** (FPD-2) without (red solid curve) and with HClO (red dash curve) in pH 5.0 PBS buffered water.

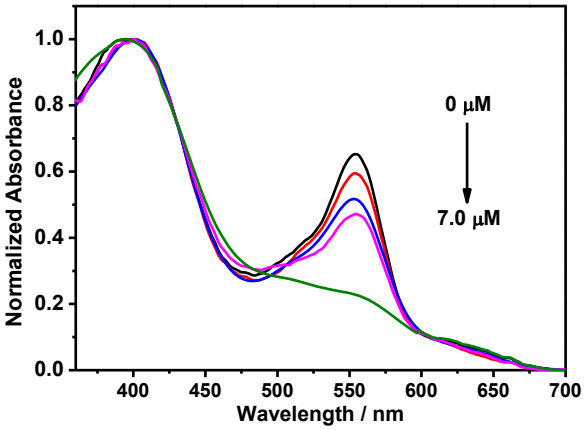

Figure S8. Normalized absorbance spectra of **FPD** (FPD-3, 12 μg/mL) under different concentration of HClO (0, 1.0, 2.0, 3.0, 7.0 μM) (pH = 5.0, buffered solution).

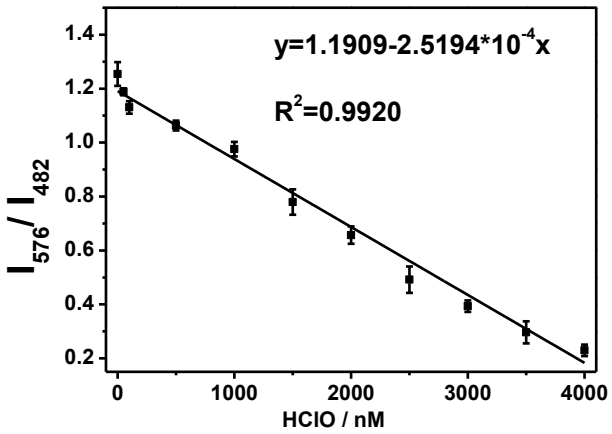

Figure S9. The ratiometric fluorescence intensity (I_{576}/I_{482}) versus HClO concentration (0-4000 nM).

Determination of the detection limit:

Fluorescence:

First the calibration curve was obtained from the plot of ratio fluorescence intensity (I_{576}/I_{482}) as a function of HClO concentration. The regression curve equation was then obtained for the lower concentration part.

The detection limit = $3 \times \sigma bi / m$

where m is the slope of the curve equation, and σbi represents the standard deviation for the fluorescence ratiometric intensity (I_{576}/I_{482}) of **FPD** (FPD-3) in the absence of HClO.

$I_{576} / I_{482} = 1.1575 - 2.5194 \times 10^{-4} \times [HClO]$

LOD = $3 \times 0.00043 / (2.5194 \times 10^{-4}) = 5.1$ nM.

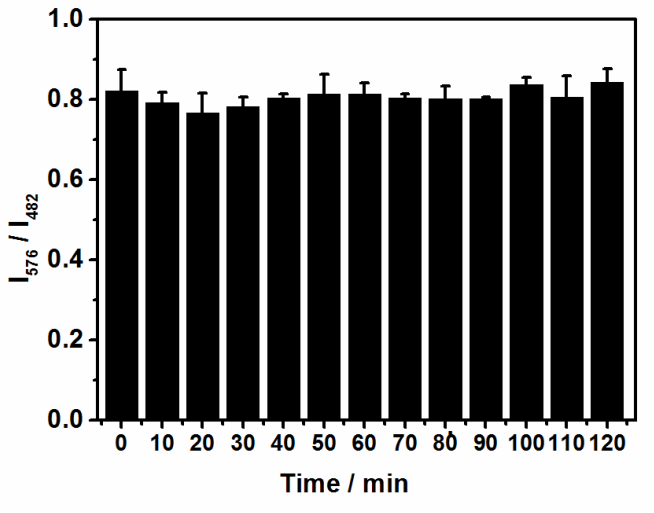

Figue S10. Fluorescence intensity changes (I_{482}/I_{576}) of **FPD** (FPD-3, 12 μg/mL) under a continuous 365 nm UV lamp irradiation (2.8 mW/cm^2).

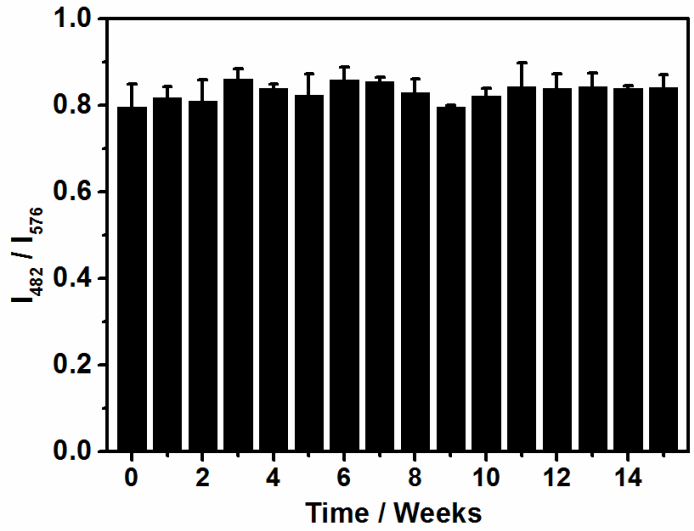

Figure S11. Fluorescence long-term photostability of **FPD** (FPD-3, 12 μg/mL) under ambient temperature and kept in the dark.

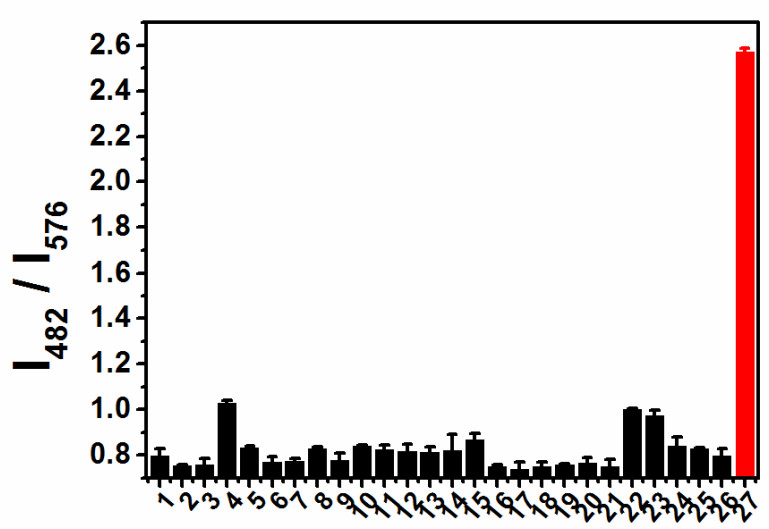

Figure S12. The ratiometric fluorescence intensity (I_{576}/I_{482}) response of **FPD** (FPD-3, 12 μg/mL) toward various analytes (50 μM for other). (1) blank, (2) Zn^{2+}, (3) Mg^{2+}, (4) Fe^{3+}, (5) Ni^{2+}, (6) Co^{2+}, (7) Hg^{2+}, (8) Ag^{+}, (9) Ca^{2+}, (10) Fe^{2+}, (11) GSH, (12) Hcy, (13) Cys, (14) S^{2-}, (15) SO_3^{2-}, (16) NO_2^{-}, (17) NO_3^{-}, (18) HSO_4^{2-}, (19) SO_4^{2-}, (20) HPO_4^{2-}, (21) $H_2PO_4^{-}$, (22) HO•, (23) *t*-BuO•, (24) $^1O_2$, (25) H_2O_2, (26) *t*-BuOOH, (27) HClO (3 μM).

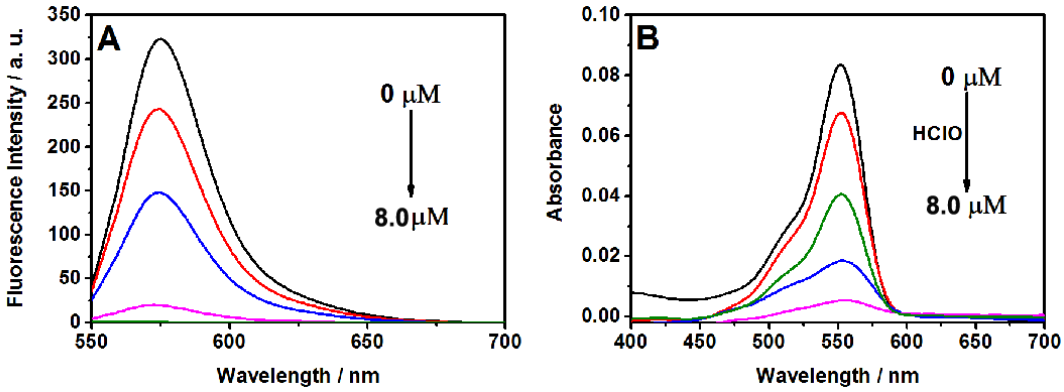

Figure S13. (A) Fluorescence spectra of RHB (2 μM) in pH 5.0 PBS buffered water in the presence of different concentration of HClO (0 μM, 1.0 μM, 2.0 μM, 4.0 μM, 8.0 μM). (B) The absorbance spectra of RHB (2.0 μM) in pH 5.0 PBS buffered water in the presence of different concentration of HClO (0 μM, 1.0 μM, 2.0 μM, 4.0 μM, 8.0 μM);

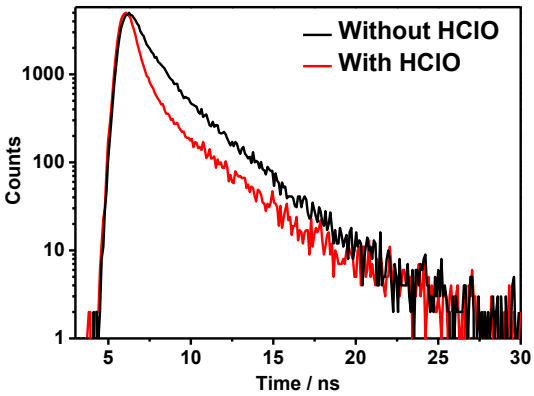

Figue S14. Fluorescence decay curves of RHB (2 μM) at 576 nm in pH 5.0 PBS buffered water without and with HClO (8.0 μM).

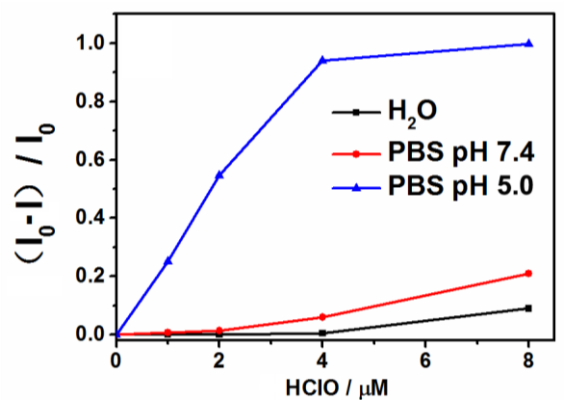

(A)

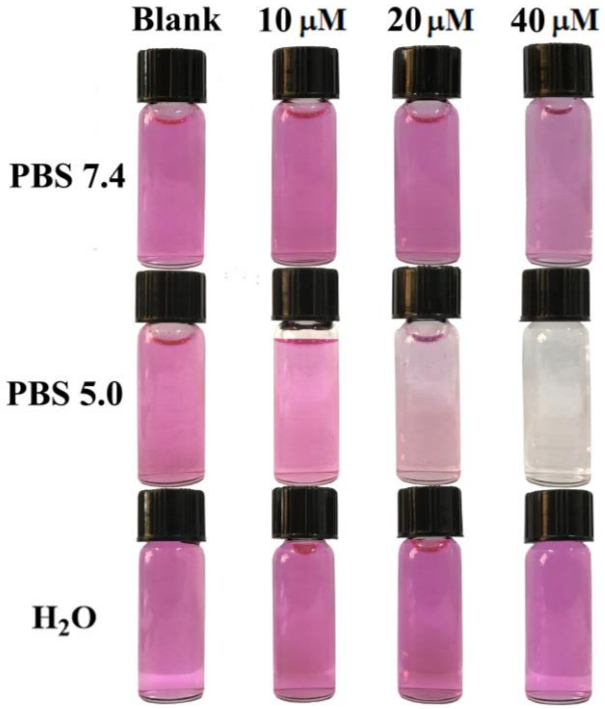

(B)

Figure S15. (A) The fluorescence change ($(I-I_0)/I_0$) of RHB (2 μM) at 576 nm in different environment versus HClO concentration (0-8.0 μM) (I_0 indicates the fluorescence of free RHB and I indicates the fluorescence of RHB after introduction of corresponding concentration HClO). (B) The color changes of RHB (20 μM) in the presence of different concentration HClO under different aqueous solution containing PBS (10 mM, pH = 7.4 and pH = 5.0) and water.

Note: In order to clearly visualize the experimental results of the Figure S15B, the concentration of RHB and HClO have been enlarged ten times than native concentration.

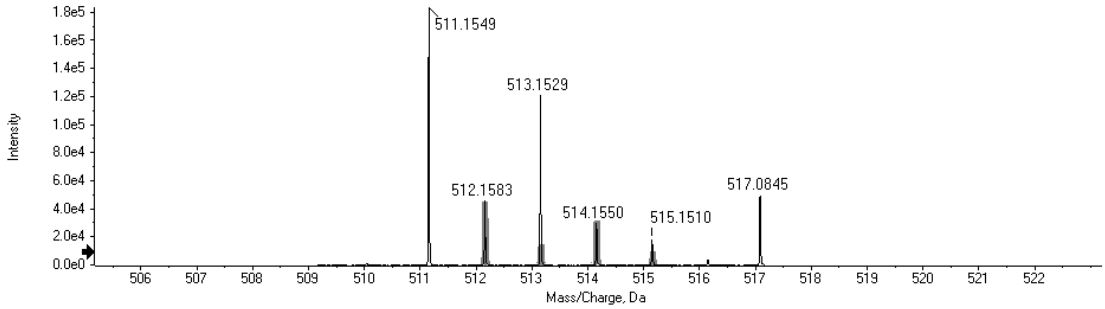

Figure S16. Mass spectrum of **RHB-HClO**. MS(ESI): m/z 511.1549 $[M+H]^+$.

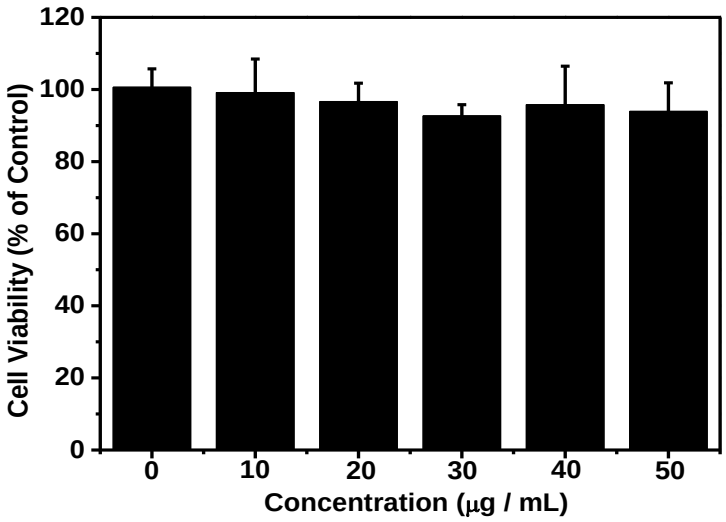

Figure S17. Cell viability for Hela cells in the presence of the probe **FPD** (FPD-3) at varied concentrations. The results are the mean standard deviation of eight separate measurements.

Table S3. Comparison of the recently reported HClO fluorescent probes

Probe	Method	Detection limit/nM	Reaction time	Solution	Imaging application of lysosome
Hypo-SiF[1]	Turn-on Fluorescent	--	within 80 s	PBS (pH 7.4, 0.5% DMF)	--
TP-HOCl1[2]	Turn-on Fluorescent	16.6	within seconds	PBS (pH 7.4, 50% EtOH)	lysosome
NR[3]	Ratiometric	14.5	within seconds	PBS (pH 5.0, 30% EtOH)	lysosome
Ir-Fc[4]	Turn-on Fluorescent	93.3	within seconds	PBS (pH 7.4, 50% EtOH)	--
NR-HOCl[5]	Turn-on Fluorescent	--	within seconds	PBS (pH 7.4, 1 % EtOH)	--
HCSe[6]	Turn-on Fluorescent	7.98	within 2 min	PBS (pH 7.4, 1 % CH_3CN)	--
Lyso-1[7]	Turn-on Fluorescent	60	within 5 min	PBS (pH 7.4, 10 % EtOH)	lysosome
HKOCl-3[8]	Turn-on Fluorescent	0.33	within 1 min	PBS (pH 7.4, 0.1 % DMF)	lysosome
Ptz-AO[9]	Turn-on Fluorescent	2.7	within 5 seconds	PBS (pH 5.0)	--
Naph-Rh[10]	Ratiometric Fluorescent	100	within seconds	PBS (pH 6, 30% EtOH))	--
PMN-TPP[11]	Ratiometric Fluorescent	430	within seconds	PBS (pH 7.4, 0.5% DMSO and 1 mM Triton X-100)	--
BFClO[12],	Ratiometric Fluorescent	10.6	within 10 s	PBS (pH 7.4, 50% EtOH))	lysosome
Ru-Fc[13]	Turn-on Fluorescent	38.6	within seconds	PBS (pH 7.4, 25% EtOH))	lysosome
Lyso-HA[14]	Ratiometric Fluorescent	110	within seconds	PBS (pH 7.4, 30% DMSO)	lysosome

This work	Ratiometric Fluorescent	5.1	within 30 s	PBS (pH 5.0)	lysosome

1. Best, Q. A., Sattenapally, N., Dyer, D. J., Scott, C. N., McCarroll, M. E. (2013). pH-dependent Si-fluorescein hypochlorous acid fluorescent probe: spirocycle ring-opening and excess hypochlorous acid-induced chlorination. J. Am. Chem. Soc., 135(36), 13365-13370.

2. Yuan, L., Wang, L., Agrawalla, B. K., Park, S. J., Zhu, H., Sivaraman, B., Peng, J., Xu, Q. H., Chang, Y. T. (2015). Development of targetable two-photon fluorescent probes to image hypochlorous acid in mitochondria and lysosome in live cell and inflamed mouse model. J. Am. Chem. Soc., 137(18), 5930-5938.

3. Shen, S. L., Ning, J. Y., Zhang, X. F., Miao, J. Y., Zhao, B. X. (2017). Through-bond energy transfer-based ratiometric fluorescent probe for the imaging of HOCl in living cells. Sens. Actuators. B, 244, 907-913.

4. Zhang, F., Liang, X., Zhang, W., Wang, Y. L., Wang, H., Mohammed, Y. H., Song, B., Zhang, R., Yuan, J. (2017). A unique iridium (III) complex-based chemosensor for multi-signal detection and multi-channel imaging of hypochlorous acid in liver injury. Biosens. Bioelectron., 87, 1005-1011.

5. Zhou, X., Lai, R., Beck, J. R., Li, H., Stains, C. I. (2016). Nebraska Red: a phosphinate-based near-infrared fluorophore scaffold for chemical biology applications. Chem. Commun., 52(83), 12290-12293.

6. Liu, S. R., Wu, S. P. (2013). Hypochlorous acid turn-on fluorescent probe based on oxidation of diphenyl selenide. Org. let., 15(4), 878-881.

7. Jiao, X., Liu, C., Wang, Q., Huang, K., He, S., Zhao, L., Zeng, X. (2017). Fluorescence probe for hypochlorous acid in water and its applications for highly lysosome-targetable live cell imaging. Anal. Chim. Acta, 969, 49-56.

8. Hu, J. J., Wong, N. K., Lu, M. Y., Chen, X., Ye, S., Zhao, A. Q., Yang, D. (2016). HKOCl-3: a fluorescent hypochlorous acid probe for live-cell and in vivo imaging and quantitative application in flow cytometry and a 96-well microplate assay. Chem. Sci., 7(3), 2094-2099.

9. Liang, L., Liu, C., Jiao, X., Zhao, L., Zeng, X. (2016). A highly selective and sensitive photoinduced electron transfer (PET) based HOCl fluorescent probe in water and its endogenous imaging in living cells. Chem. Commun., 52(51), 7982-7985.

10. Zhang, Y. R., Meng, N., Miao, J. Y., Zhao, B. X. (2015). A Ratiometric Fluorescent Probe Based on a Through-Bond Energy Transfer (TBET) System for Imaging HOCl in Living Cells. Chem. Eur. J., 21(52), 19058-19063.

11. Huang, Y., Zhang, P., Gao, M., Zeng, F., Qin, A., Wu, S., Tang, B. Z. (2016). Ratiometric detection and imaging of endogenous hypochlorite in live cells and in vivo achieved by using an aggregation induced emission (AIE)-based nanoprobe. Chem. Commun., 52(45), 7288-7291.

12. Zhang, Z.; Fan, J.; Cheng, G.; Ghazali, S.; Du, J.; Peng, X., Fluorescence completely separated ratiometric probe for HClO in lysosomes. Sens Actuators B 2017, 246, 293-299.

13. Cao, L.; Zhang, R.; Zhang, W.; Du, Z.; Liu, C.; Ye, Z.; Song, B.; Yuan, J., A

ruthenium(II) complex-based lysosome-targetable multisignal chemosensor for in vivo detection of hypochlorous acid. Biomaterials, 2015, 68, 21-31.
14. Ren, M.; Deng, B.; Zhou, K.; Kong, X.; Wang, J.-Y.; Xu, G.; Lin, W., A lysosome-targeted and ratiometric fluorescent probe for imaging exogenous and endogenous hypochlorous acid in living cells. J Mater Chem B 2016, 4 (27), 4739-4745.